

# Improved model for the analysis of air fluorescence induced by electrons

F. Arqueros, F. Blanco and J. Rosado

*Facultad de Ciencias Físicas, Universidad Complutense de Madrid, E-28040 Madrid, Spain*

---

## Abstract

A model recently proposed for the calculation of air-fluorescence yield excited by electrons is revisited. Improved energy distributions of secondary electrons and a more realistic Monte Carlo simulation including some additional processes have allowed us to obtain more accurate results. The model is used to study in detail the relationship between fluorescence intensity and deposited energy in a wide range of primary energy (keVs - GeVs). In addition, predictions on the absolute value of the fluorescence efficiency in the absence of collisional quenching will be presented and compared with available experimental data.

*Key words:* air-fluorescence, fluorescence telescopes

*PACS:* 34.50.Gb, 34.50.Gs, 34.50.Bw

---

## 1. Introduction

The accuracy in the energy determination of ultra-high energy cosmic rays using the fluorescence technique is presently limited by the uncertainty in the air-fluorescence yield. In order to improve the accuracy of this fundamental parameter, several laboratory measurements are being performed [1,2,3,4,5,6,7,8]. On the other hand, progress on the theoretical understanding of the various processes leading to the air-fluorescence emission is being carried out. At high pressure ( $\gtrsim 1$  Torr) and high electron energy ( $\gtrsim 1$  keV) most of the fluorescence light is generated by low energy secondary electrons arising from  $N_2$  ionization [9]. A simple model which accounts for the contribution of secondary electrons to the fluorescence yield of the  $N_2$  2P system ( $C^3\Pi_u \rightarrow B^3\Pi_g$ ) has been recently published [9]. Using the above model, the total fluorescence yield has been computed for the first time at high electron energies in [10].

Since fluorescence is mainly generated by sec-

ondary electrons, their energy distribution is a key parameter. Previous results [9,10] were obtained using the analytical energy distribution given by Opal et al. [11] which has been experimentally checked at low energy (below a few keVs). Unfortunately, the extrapolation of this formula to higher energies is not suitable to account for the energy distribution of delta rays properly. In the present paper, a new analytical approach valid in the whole energy interval (eV - GeV) is used. Preliminary updated results of our model using this energy spectrum together with improved molecular parameters and a more realistic Monte Carlo simulation are presented in this paper.

Proportionality between fluorescence intensity and the energy deposited by the primary electron is usually assumed. Experimental results seem to support this assumption, at least, in small energy intervals. Recently the MACFLY collaboration has extended this experimental test to a large energy range, 1.5 MeV - 50 GeV, finding proportionality within their experimental errors of about 15% [4].

However, from a theoretical point of view this proportionality is not obvious. The excitation of the fluorescence emission is strongly peaked at low energies, in particular for the 2P system of nitrogen and therefore the ratio of fluorescence emission and deposited energy is strongly dependent on the spectrum of low energy secondaries. In principle, this spectrum depends on both the primary energy and the distance from the primary interaction, and thus, this proportionality has to be demonstrated with a detailed analysis.

## 2. The model

The model described in [9,10] shows that the total number of photons of the  $v - v'$  band generated by an electron per unit path length in a thin target can be expressed by

$$\varepsilon_{vv'}(P) = N \frac{1}{1 + P/P'_v} \{ \sigma_{vv'}(E) + \alpha_{vv'}(E, P) \sigma_{ion}(E) \}. \quad (1)$$

$N$  is the number of nitrogen molecules per unit volume. Collisional de-excitation (quenching) is taken into account by the well-known Stern-Volmer factor which depends on the characteristic pressure  $P'_v$ . As shown in this expression, the fluorescence intensity is a sum of two contributions: a) direct excitation of  $v - v'$  band by the primary electron, given by the optical cross section  $\sigma_{vv'}$  and b) contributions from secondary electrons arising from molecular ionizations, proportional to the ionization cross section.

The optical cross section is defined by

$$\sigma_{vv'} = \sigma_v \frac{A_{vv'}}{\sum_{v'} A_{vv'}}, \quad (2)$$

where  $\sigma_v$  is the cross section for electron excitation (ionization) of molecular nitrogen in the ground state to the upper  $v$  level of an excited electronic state of  $N_2$  ( $N_2^+$ ), and  $A_{vv'}$  are the  $v - v'$  radiative transition probabilities (Einstein coefficients). Therefore the optical cross sections  $\sigma_{2P(0-0)}$ ,  $\sigma_{1N(0-0)}$  used below are associated to the emission of a 337 nm and 391 nm photon respectively induced by electron collision on a  $N_2$  molecule.

For high pressures ( $\gtrsim 1$  Torr) and energies ( $\gtrsim 1$  keV) the contribution from secondary electrons is dominant for generation of 2P fluorescence and relevant for the 1N bands. The parameter  $\alpha_{vv'}$  in (1) represents the average number of  $v - v'$  photons generated inside the observation volume as a result of a primary ionization in the absence of quenching.

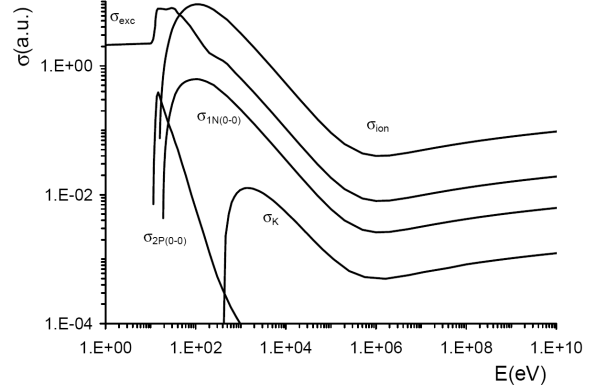


Fig. 1. Cross sections (atomic units) involved in the emission of air fluorescence as a function of energy. Cross section  $\sigma_{exc}$  accounts for all excitation processes without emission of a secondary electron. Cross section  $\sigma_{ion}$  accounts for all processes leading to the emission of a secondary electron. The cross section for the ejection of a K shell electron  $\sigma_K$  is shown for comparison. The optical cross sections for the excitation of the 1N (0-0) and 2P (0-0) bands are also shown.

The evaluation of  $\alpha_{vv'}$  has to be carried out by a Monte Carlo simulation which takes into account the various generations of secondary electrons produced after a primary ionization. The  $\alpha_{vv'}$  parameter turns out to be a function of primary energy  $E$ , pressure  $P$  and the geometrical features of the observation region.

Next we will describe the molecular parameters used in our simulation. In the first place, figure 1 shows the nitrogen cross section versus energy for various  $e^-$ -molecule interaction processes of interest in our problem. The cross section for molecular excitation  $\sigma_{exc}$  accounts for all excitation processes without emission of a secondary electron. On the other hand, the ionization cross section  $\sigma_{ion}$  accounts for all processes leading to the emission of a secondary electron and can be described at large energy by the Born-Bethe function. At high energy only optically allowed transitions, also well described by a Born-Bethe function, contribute and therefore  $\sigma_{exc}$  is proportional to  $\sigma_{ion}$ . The cross section for the ejection of a K shell electron  $\sigma_K$  is shown for comparison. Figure 1 also shows the optical cross sections (2) for the excitation of the 2P (0-0) and 1N (0-0) bands of  $N_2$  and  $N_2^+$  respectively. At low energy, experimental values have been used (see [10] for references) and at high energies  $\sigma_{1N(0-0)}$  has been extrapolated using the Born-Bethe function. For all cross sections the density correction at high energies [10,12,13] has been applied.

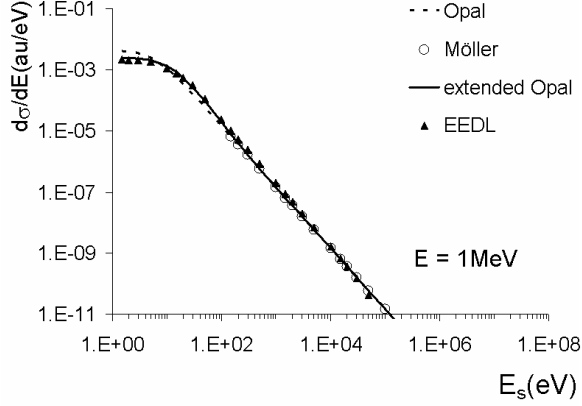


Fig. 2. Energy spectrum of secondary electrons emitted in a primary ionization induced by an electron of energy 1 MeV. The Opal formula is not able to reproduce the energy spectrum of delta rays (Möller scattering). The extended Opal formula used in this work fits properly the Möller spectrum. The values of the EEDL database are also shown for comparison. In ordinates the absolute value of the differential cross section in atomic units per eV is represented.

Another ingredient of the model is the energy lost by the electrons in each collision process. For molecular excitation (without electron ejection) an average value of  $\langle E_{exc} \rangle = 8.5$  eV has been estimated. In an ionization process the lost kinetic energy (primary and secondary electrons) equals the  $N_2$  ionization potential,  $I = 15.5$  eV, plus the excitation energy of the ion, for which an average value of  $\langle E_{exc}^{ion} \rangle = 1.3$  eV has been estimated at low energies from available data. At large energy K-shell ionization is also taken into account with a relative probability given by the corresponding cross section. In this case the kinetic energy is reduced by 410 eV (K-shell binding energy). As a result  $\langle E_{exc}^{ion} \rangle$  increases up to 5 eV.

In the present calculations the tracks of secondary electrons have been simulated using available angular cross section for the various individual interaction processes, including elastic  $e^-$ -molecule collisions. Other processes like generation of X ray from molecular de-excitation and bremsstrahlung by high energy electrons have also been included in our simulation although the final results are nearly independent on these processes.

As already mentioned, the total fluorescence emission is very sensitive to the energy spectrum of secondary electrons. At low energy the analytical expression proposed by Opal et al. fits accurately experimental results. At high primary energies, for which no experimental data

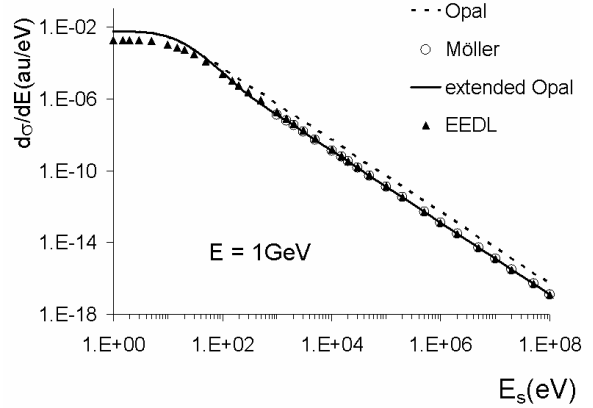


Fig. 3. Same as figure 2 for 1 GeV primary energy.

are published, precise calculations are described by Seltzer [12,13]. Numerical results for any atom are available in EEDL databases [13,14]. Instead of implementing these databases in our simulation, we looked for an analytical expression for the energy spectrum in the whole energy range for both primary and secondary electrons. The desired function must fulfill several requirements: a) it has to behave as the Opal formula at low primary energy; b) at high  $E$  the function has to account for the well known energy spectrum of delta rays, c) the integral of the differential cross section has to give the total ionization cross section and d) the assumed function must be consistent with the collision energy loss given by the Bethe-Bloch theory for electrons.

In this work a new analytical formula has been used which properly accounts for the above four conditions. Details on this analytical approach will be given in a paper in preparation. In figures 2 and 3 the energy spectrum of secondary electrons predicted by this “extended” Opal formula used in the work is compared with other available data for primary electrons of 1 MeV and 1 GeV respectively.

Fulfilment of requirement d) can be easily checked as follows. The energy loss per unit electron path length in air, assuming  $N_{air}$  molecules per unit volume, is closely related with the mean value of the energy distribution of secondary electrons by the following relation

$$\frac{dE}{dx} = N_{air} \{ \langle E_{dep}^0 \rangle + \langle E_s \rangle \} \sigma_{ion}(E), \quad (3)$$

where  $\langle E_s \rangle$  is the mean value of the energy distribution of secondary electrons at a given  $E$  value and

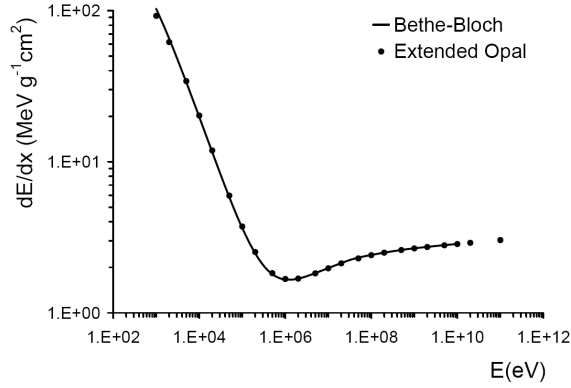


Fig. 4. Energy loss of electrons per unit path length versus primary energy. Continuous line represents the calculated values from equation (3) using the average energy of the extended Opal formula. Black dots are the values from the Bethe-Bloch formula. In both cases the medium is air at atmospheric pressure.

$$\langle E_{dep}^0 \rangle = \langle E_{exc} \rangle \frac{\sigma_{exc}}{\sigma_{ion}} + I + \langle E_{exc}^{ion} \rangle, \quad (4)$$

represents the average value of the energy deposited in the medium by the primary electron per primary ionization process.

In Figure 4 the energy loss calculated from expression (3) using the  $\langle E_s \rangle$  value from our energy distribution of secondary electrons is represented, showing full agreement with the Bethe-Bloch formula [15].

### 3. Results

In this section we will present results on the various parameters of interest for the interpretation of the air fluorescence measurements. In our simulation the observation region has been assumed to be a sphere of radius  $R$  with center in the interaction point of the primary electron. Assuming a fixed temperature, both fluorescence intensity and deposited energy turn out to be basically dependent on the product  $PR$ , that is, on the number of interactions inside the observation region. In fact, due to the density correction at very large energies, for a given  $PR$  value, the above parameters are slightly dependent on pressure. However, the corresponding deviation is not significant inside the range 100 - 760 Torr.

The energy deposited by the primary electron per unit path length can be calculated from the average energy deposited by secondary electrons  $\langle E_{dep} \rangle$  as

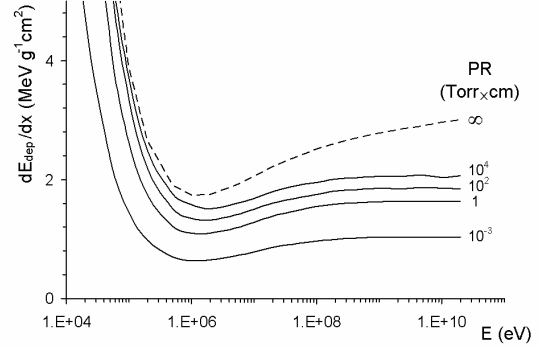


Fig. 5. Energy deposited by a primary electron per unit path length versus primary energy for several values of  $PR$  (continuous lines). For very high  $PR$  value deposited energy equals the energy loss of the primary electron predicted by the Bethe-Bloch theory (broken line).

$$\frac{dE_{dep}}{dx} = N_{air} \{ \langle E_{dep}^0 \rangle + \langle E_{dep} \rangle \} \sigma_{ion}(E). \quad (5)$$

Note that this equation is the same as (3) replacing  $\langle E_s \rangle$  by  $\langle E_{dep} \rangle$ . The value of  $\langle E_{dep} \rangle$  has been obtained from our Monte Carlo simulation. Figure 5 shows the energy deposited per unit path length versus primary energy for several  $PR$  values. We have checked that, as expected, the deposited energy for an unlimited medium,  $PR \rightarrow \infty$ , equals the energy loss predicted by the Bethe-Bloch theory.

The fluorescence efficiency  $\Phi_{vv'}$ , defined as the ratio between the number of fluorescence photons emitted in a given  $v - v'$  molecular band and the deposited energy is a fundamental parameter. Combining equations (1) and (5), the following useful relation can be obtained:

$$\Phi_{vv'}^0 = \frac{N}{N_{air}} \times \frac{\frac{\sigma_{vv'}}{\sigma_{ion}} + \alpha_{vv'}}{\langle E_{dep}^0 \rangle + \langle E_{dep} \rangle}, \quad (6)$$

where  $\Phi_{vv'}^0$  is the fluorescence efficiency in the absence of collisional quenching and thus related with  $\Phi_{vv'}$  by

$$\Phi_{vv'} = \Phi_{vv'}^0 \frac{1}{1 + P/P_v}. \quad (7)$$

The values of  $\alpha_{vv'}$  and  $\Phi_{vv'}^0$  have been computed for the 2P (0-0) and 1N (0-0) bands, for which accurate experimental results of the corresponding cross sections are available. Figures 6 and 7 show  $\Phi^0$  against  $E$  for several values of  $PR$  while in figures 8 and 9 the dependence of  $\Phi^0$  versus  $PR$  is represented for various energies.

These figures show several interesting features. In the first place, for high energy (beyond the keV range), and for observation regions larger than

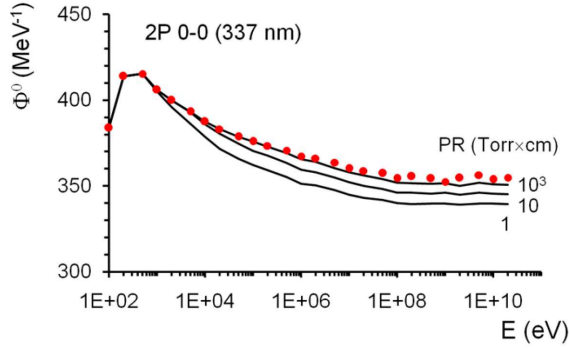


Fig. 6. Fluorescence efficiency for the 2P (0-0) band in the absence of collisional quenching against primary energy for several values of  $PR$  (continuous lines). Circles represent the result for a very large medium.

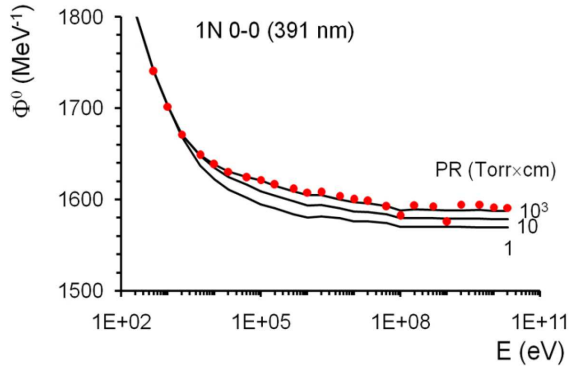


Fig. 7. Same as figure 6 for the 1N (0-0) transition.

about 1 Torr $\times$ cm,  $\Phi^0$  is nearly constant. Nevertheless a smooth dependence on primary energy is found. The value of  $\Phi^0$  decreases with primary energy about 10% in the range 1 keV - 1 MeV and 4% in the interval 1 MeV - 20 GeV for the 337 nm band (figure 6). For the 391 band the corresponding decreasing is about 6% for the interval 1 keV - 1 MeV and 1% for 1 MeV - 20 GeV (figure 7). On the other hand a smooth growing of  $\Phi^0$  with  $PR$ , smaller than 2% in the range 10 - 1000 Torr $\times$ cm, is also found for energies larger than 1 MeV (figures 8 and 9). At lower energy and/or region size the fluorescence is clearly not proportional to the deposited energy.

The real number of photons detected per unit of deposited energy  $\Phi$  can be calculated from equation (7) using the corresponding  $P'_v$  value. Unfortunately there are significant disagreements in the available experimental data of collisional quenching in air. Therefore the comparison of the absolute value of the efficiency with experimental data is not straightforward. On the other hand, some experiments only

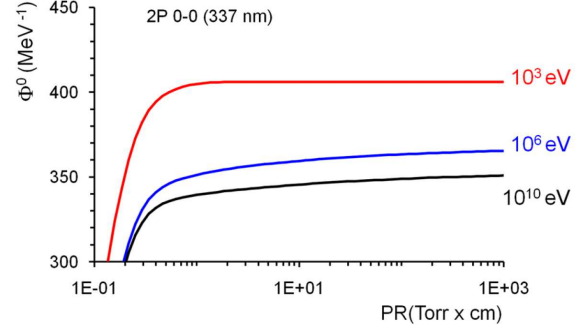


Fig. 8. Fluorescence efficiency for the 2P (0-0) band in the absence of collisional quenching against the size of the observation region  $PR$  for several primary energies.

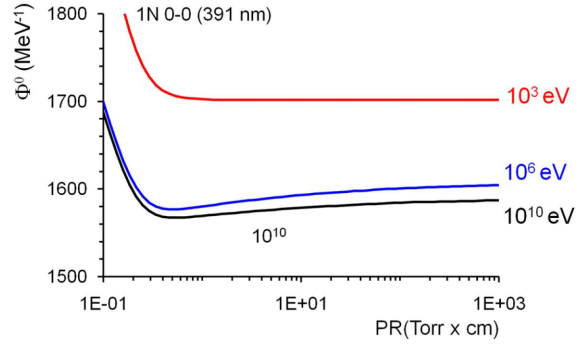


Fig. 9. Same as figure 8 for the 1N (0-0) transition.

provide a measure of the total fluorescence in a wide spectral range including most of the molecular transitions. In addition, very often the fluorescence yield is given in units of photons per meter.

The fluorescence efficiency at zero pressure for a reference molecular band (e.g. the 337 nm band) can be inferred from the number of photons per unit electron path length  $\varepsilon_\lambda$  emitted in a given wavelength interval at a given pressure by

$$\Phi_{337}^0 = \frac{\varepsilon_\lambda}{dE_{dep}/dx} \frac{I_{337}}{I_\lambda} \left( 1 + \frac{P}{P'_{337}} \right), \quad (8)$$

where the ratio between the fluorescence intensity for the 337 nm band  $I_{337}$  and that for a broad wavelength interval  $I_\lambda$  can be calculated from the Franck-Condon factors, Einstein coefficients and  $P'_v$  values, as explained in detailed in ref. [10]. For the comparisons shown below the energy deposited per unit path length  $dE_{dep}/dx$  has been obtained from our MC simulations (figure 5) assuming for all experiments a typical  $PR$  value of 1600 Torr $\times$ cm. Notice that this parameter depends on  $PR$  very smoothly (around 6% variation in the interval 300 -

Table 1

Parameters for the calculation of  $\Phi_{337}^0$  experimental data at atmospheric pressure. Experiment reference, electron energy, spectral bandwidths and measured number of air-fluorescence photons per meter are displayed in columns one to four. Fifth column shows the deposited energy per meter obtained from our simulations. The sixth one gives the total fluorescence efficiency at atmospheric pressure in the spectral interval. The ratio of the 337 nm band intensity to total intensity is shown in next two columns (7 and 8). Ratios have been calculated assuming the set of  $P'_v$  values given either by references [16] ( $P'_P$  column) or [5] ( $P'_A$  column). Next two columns show inferred values of  $\Phi_{337}^0$  assuming the above mentioned  $P'_v$  values. Column eleven shows the  $\Phi_{337}^0$  result reported by the experiment. Last column shows the preliminary theoretical results presented in this work. Bolded figures are those inferred from our calculations.

Experiment	$E$	$\lambda$	$\varepsilon_\lambda$	$dE_{dep}/dx$	$\Phi_\lambda$	$I_{337}/I_\lambda$		$\Phi_{337}^0 [\text{MeV}^{-1}]$			
	[MeV]	[nm]	[m <sup>-1</sup> ]	[MeVm <sup>-1</sup> ]	[MeV <sup>-1</sup> ]	$P'_P$	$P'_A$	$P'_P$	$P'_A$	reported	this work
Nagano et al.	0.85	337	1.021	<b>0.18</b>	<b>5.67</b>	1	1	<b>440</b>	<b>370</b>	272	<b>365</b>
FLASH 07	$2.8 \times 10^4$	300 - 420	5.06	<b>0.24</b>	<b>20.8<sup>†</sup></b>	<b>0.28</b>	<b>0.27</b>	<b>460</b>	<b>370</b>		<b>350</b>
MACFLY	$1.5 - 5.0 \times 10^4$	290 - 440			17.6	<b>0.27</b>	<b>0.26</b>	<b>380</b>	<b>290</b>	174	<b>365 - 352</b>

<sup>†</sup> Value reported by FLASH.

3000 Torr×cm). For the following discussion we will use  $P'_v$  measurements very recently published by the AIRFLY collaboration [5] and those obtained from deactivation rate constants N-N and N-O measured by Pancheshnyi et al. [16] (see also [10]).

We have compared our theoretical  $\Phi_{337}^0$  value with some available experimental data. For instance Nagano et al. [1], working at an average energy of about 0.85 MeV, reports a value of 272 MeV<sup>-1</sup> significantly smaller than our predictions. However from their measurement of 1.021 photons (337 nm) per meter at atmospheric pressure, results from (8) of 440 or 370 MeV<sup>-1</sup> are found by using  $P'_v$  values of [16] or [5] respectively, the last one in very good agreement with our predicted value of 365 MeV<sup>-1</sup> (see table 1). This discrepancy can be explained by comparing the  $P'_{337}$  value of 14.4 Torr reported by [1] with those of 9.8 and 11.9 Torr from [16] and [5] respectively. This simple exercise shows that the result of the comparison is strongly dependent on the chosen  $P'_{337}$  value.

Another interesting example is the comparison with the measurement recently reported by the FLASH collaboration at 28 GeV [3]. In this case we use their 5.06 photons/m for the whole fluorescence spectrum in the wavelength range 300 - 420 nm. The contribution to the total intensity  $I_\lambda$  of the Gaydon-Herman bands measured by AIRFLY [5] has been included. The inferred  $\Phi_{337}^0$  results are 453 and 353 MeV<sup>-1</sup> using  $P'_{337}$  values of [16] or [5] respectively (see table 1). Again the second one is in very good agreement with our predictions. Note that, as shown in the table, the factor  $I_{337}/I_\lambda$  is only weakly dependent on the  $P'_v$  set used.

Finally the  $\Phi_{337}^0$  result reported by MACFLY [4]

of 174 MeV<sup>-1</sup>, constant in the range 1.5 MeV - 50 GeV, is smaller than our predictions. Notice that the value  $P'_{337} = 19.4$  Torr of [4] is larger than those of [16] or [5]. In fact, following the above described procedure a  $\Phi_{337}^0$  value of 380 or 290 MeV<sup>-1</sup>, using [16] or [5] respectively, would be inferred from the MACFLY result of  $\Phi_\lambda = 17.6$  photons/MeV at atmospheric pressure in the spectral interval 290 - 440 nm.

#### 4. Conclusions

An improved model for the air-fluorescence emission has been used to analyze in detail the relationship between fluorescence intensity and deposited energy. For primary energies larger than a few keV and assuming observation regions over 10 Torr×cm nitrogen fluorescence is nearly proportional to deposited energy. A smooth decrease of  $\Phi^0$  of about 10% in the range 1 keV - 1 MeV and 4% in the interval 1 MeV - 10 GeV for the 2P system is found. Taking into account that the contribution of the energy released by an extensive air shower by electrons with energy smaller than 1 MeV is only of about 22% [17], the above smooth dependence of efficiency on primary energy has no impact on the calibration of fluorescence telescopes. Nevertheless very precise laboratory measurements (better than 10%) of the fluorescence yield in the range keVs - GeVs could observe this small effect.

The absolute value of the fluorescence efficiency for the 337 nm band computed in this work has been compared with some experimental results. The comparison was carried out by reducing experimental values of number of photons per meter at atmo-

spheric pressure to  $\Phi_{337}^0$  using quenching data from other authors. In general we found a good agreement, in particular when using quenching parameters from AIRFLY.

Our improved energy distribution of secondaries (consistent with the energy loss predicted by the Bethe-Bloch formula) has lead us to demonstrate quantitatively that fluorescence intensity is basically proportional to deposited energy. On the other hand, uncertainties in the absolute values of theoretically predicted  $\Phi_{vv}^0$ , quantities are larger because these are limited by the accuracy of the assumed molecular parameters involved in the calculations.

## 5. Acknowledgements

This work has been supported by the Spanish Ministry of Science and Education MEC (Ref.: FPA2006-12184-C02-01) and “Comunidad de Madrid” (Ref.: 910600). J. Rosado acknowledges a PhD grant from “Universidad Complutense de Madrid”.

## References

- [1] M. Nagano et al., *Astropart. Phys.* 22 (2004) 235.
- [2] J. W. Belz et al., *Astropart. Phys.* 25 (2006) 129.
- [3] R. Abbasi et al., *Astropart. Phys.* 29 (2008) 77.
- [4] P. Colin et al., *Astropart. Phys.* 27 (2007) 317.
- [5] M. Ave et al., *Astropart. Phys.* 28 (2007) 41.
- [6] G. Lefeuve et al., *Nucl. Inst. Meth. A* 578 (2007) 78.
- [7] T. Waldenmaier et al., arXiv:0709.1494 [astro-ph]; submitted to *Astropart. Phys.*
- [8] J. Rosado et al., these Proceedings.
- [9] F. Blanco and F. Arqueros, *Phys. Lett A* 345 (2005) 355.
- [10] F. Arqueros et al., *Astropart. Phys.* 26 (2006) 231.
- [11] C. B. Opal, E. C. Beaty, W.K. Peterson, *At. Data* 4 (1972) 209.
- [12] S. M. Seltzer, “Cross Sections for Bremsstrahlung Production and for Electron Impact Ionization”, in *Monte Carlo Transport of Electrons and Photons*, Chapt.4 (T.M.Jenkins et al., eds.)(Plenum Press, N.Y. 1988).
- [13] S. T. Perkins et al., “Tables and Graphs of Electron-Interaction Cross Sections from 10 eV to 100 GeV Derived from the LLNL Evaluated Electron Data Library (EDDL)”, UCRL-50400 Vol. 31 (November 1991).
- [14] EEDL databases are included in GEANT4 packages or available at [www-nds.iaea.org/epdl97/](http://www-nds.iaea.org/epdl97/).
- [15] R. M. Sternheimer et al. *Phys. Rev. B* 26 (1982) 6067; <http://physics.nist.gov/PhysRefData/Star/Text/ESTAR.html>
- [16] S. V. Pancheshnyi et al., *Chemical Physics* 262 (2000) 349.
- [17] M. Risse and D. Heck, *Astropart. Phys.* 20 (2004) 661.